

Analysis of Combination Algorithms for Denoising and Contrast Enhancement Images

Irpan Adiputra Pardosi, Hernawati Gohzali
Department of Informatics, Mikroskil University, Medan, Indonesia

ARTICLE INFO

Article history:

Received November 11, 2021
Revised April 27, 2022
Accepted May 25, 2022

Keywords:

AFECDP;
Contrast Enhancement;
Denoising;
IDBP-CNN;
MADF;
TFM-CLAhe

ABSTRACT

Reducing noise and increasing image contrast is part of the purpose of enhancing image quality; instead, it will impact change the diversity of information in the image based on the Shannon entropy value. Decrease quality caused by noise salt and pepper in this research or abnormal contrast in the image causes objects in the image to become unclear. Low contrast has a major impact on image quality, including noise reduction processes affecting image information so that the quality of the reduced image becomes something to consider for large noise. Iterative Denoising and Backward Projections with CNN (IDBP-CNN) and Different Applied Median Filter (DAMF) is a good solution for denoising a large percentage of noise with good quality results image. In other research for contrast enhancement, Triangular Fuzzy Membership-Contrast Limited Adaptive Histogram Equalization (TFM-CLAHE) and Adaptive Fuzzy Contrast Enhancement Algorithm with Details Preserving (AFCEDP) is claimed to a good solution to solve low contrast of the image. Therefore, this study is to find the best combination of denoising and contrast enhancement to get good image results with step denoising followed by contrast enhancement. Based on the experimental testing is got the best combination is the DAMF + AFCEDP algorithm with an average of PSNR 35dB and an average difference Shannon entropy of 0.0130.

This work is licensed under a [Creative Commons Attribution-Share Alike 4.0](https://creativecommons.org/licenses/by-sa/4.0/)



Corresponding Author:

Irpan Adiputra Pardosi, Department of Informatics, Mikroskil University, Medan, Indonesia
Email: irpan@mikroskil.ac.id

1. INTRODUCTION

Reducing noise and increasing image contrast is part of enhancing image quality. Instead, it will impact changing the diversity of information in the image based on the Shannon entropy value [1][2][3]. Decrease quality caused by noise or abnormal contrast in the image causes objects in the image to become unclear [4][5][6], but this can happen causes many things, such as the device used creating noise or cannot produce normal contrast or it can also occur during the process of sending images through the network there is a decrease in quality due to compression in the image [7][8]. Salt and pepper is a kind of noise that is often dissolved in image processing, but on the other side, low contrast also has a major impact on image quality [9][10][11]. Large noise reduction processes affect image information so that the quality of the reduced image becomes something to consider for large noise [12][13][14]. The problem of images with noise and also low contrast, in the end, becomes an important thing to be solved so that the data processing process in the image is not hampered for the next stage either for object identification, pattern recognition, or other purposes [15][16][17][18].

Relevant research for the noise reduction process with a noise distribution percentage of 45% using the Adaptive Fuzzy Filter (AFF) algorithm with a PSNR result of 28.10 dB [13], Fuzzy Filter one of the solutions to solve denoising with big percentage [19][20] with the result still below a good image quality of 30 dB [21]. However, in 2019 research using the Iterative Denoising and Backward Projections with CNN (IDBP-CNN) algorithm was stated to be able to reduce noise up to 51% but with image quality based on

PSNR values up to 30 dB, with tests carried out ignoring the contrast of the image [22], in others research IDP with CNN has the potential for widespread clinical applications [23]. Another study to improve image quality used the Modified Decision-Based Unsymmetrical Trimmed Median Filter (MDBUTMF) algorithm substantially outperformed all existing median-based filters in terms of reducing the percentage level of Salt and pepper noise and maintaining image detail [24][25][26]. The proposed algorithm is tested against various grayscale and color images that get better Peak Signal-to-Noise Ratio (PSNR) and Image Enhancement Factor (IEF) at different noise percentages. Conducted further research by comparing the MDBUTMF algorithm, Different Applied Median Filter (DAMF), and several other methods using PSNR and Structural Similarity (SSIM) for 5 images with 50% noise. The PSNR and SSIM results of the DAMF method were 31.97 dB and 0.9285, respectively, which were the best results from the compared methods [27]. The image is said to be good if the PSNR value is above 30 dB. An image that has a PSNR value below 30 dB is said to be degraded and cannot be considered for further analysis [21][28]. However, the Median Filter process for all pixels disguises the original image, which is correct and does not need to be corrected and causes a decrease in the quality of the improved image [29][30].

While the algorithm to increase the contrast of the image uses the Gradient-Based Low Light Image Enhancement algorithm with the results of the similarity of the resulting image with the original image up to SSIM 7.0077, the impact of the implementation on low contrast images causes noise in the resulting image and when the process has repeated the quality of the resulting image decreases [31][32]. In addition, another study implemented a contrast enhancement algorithm using the Triangular Fuzzy Membership-Contrast Limited Adaptive Histogram Equalization (TFM CLAHE) algorithm, which is claimed to be able to increase image contrast with PSNR quality above 20 dB [33], which is better than the Histogram Equalization (HE) algorithm, Adaptive HE (AHE), Contrast Limited AHE (CLAHE) [34], both image quality improvement algorithms can produce images with PSNR quality above 30 dB. Similar research has been carried out to improve image contrast quality by comparing the Adaptive Fuzzy Contrast Enhancement Algorithm with Details Preserving (AFCEDP) using the same algorithm, the Adaptive Contrast Enhancement Algorithm. The difference is that without using fuzzy, AFCEDP gets better results without reducing information [35]. Image significantly [4] also compared the Adaptive Fuzzy Contrast Enhancement Algorithm With Details Preserving (AFCEDP) with 2 other types of filters and found that AFCEDP gave better results than the compared method.

Based on the reference, the research contribution is to get the best combination of the denoising and contrast enhancement algorithm between the denoising algorithm of DAMF and IDBP-CNN with contrast algorithm TFM-Clahe and AFCEDP algorithm has never been tested, so it is necessary to conduct a more in-depth study in the hope that an ideal model will be found to overcome noise and low contrast with relatively better-quality results. This research applies the method to reduce salt and pepper noise with a percentage of 45% using the Threshold = 192 value for the reference iteration process of noise reduction [36], and the contrast method is used to improve the contrast of dark low-contrast images. Analysis of combination method noise reduction and contrast enhancement measurement image quality based on MSE and PSNR values. To determine the difference in information diversity in the resulting image compared to the original image with the Shannon entropy method after the two image quality improvement processes were carried out.

2. METHOD

2.1. Iterative Denoising and Backward Projections with CNN (IDBP-CNN)

The proposed algorithm, which we call Iterative Denoising and Backward Projections (IDBP) with Convolution Neural Network (CNN), is presented in the algorithm as

Input: H, y, σ_e , denoising operator $\mathcal{D}(\cdot; \sigma)$, stopping criteria, $\mathcal{Y} = H_x + e$, such that $e \sim \mathcal{N}(0, \sigma_e^2 I_m)$ and x is an unknown signal whose prior model is specified by $\mathcal{D}(\cdot; \sigma)$

Output: \tilde{x} an estimate for x

Initialization: $\tilde{\mathcal{Y}}_0 = \text{some initialization}$, $k = 0$, δ approx.

while {stopping criterion not met} **do**

$$k = k + 1; \quad (1)$$

$$\tilde{x}_k = \mathcal{D}(\tilde{\mathcal{Y}}_k - 1; \sigma_e + \delta); \quad (2)$$

Requires a single DNN (convolution+Re-LU) for each inverse problem, as do not modify δ between iterations to get \tilde{x}_k [36]

$$\tilde{\mathcal{Y}}_k = H^\dagger y + (I_n - H^\dagger H) \tilde{x}_k; \quad (3)$$

end

$$\hat{X} = \tilde{X}_k;$$

2.2. TFM-Clahe Method

TFM-CLAHE provides automatic, image variant fuzzy clip-limit for limiting contrast and resulting in the enhanced image. The clipped portion of the histogram that surpasses the clip limit is redistributed among all histogram bins equally. The triangular fuzzy membership function (TFM) takes three values as inputs which form the minimum, maximum, and mean values of the image’s pixel intensities in the considered window and computes the fuzzy $\mu_1(Pr_\beta)$ which determines the clipping parameters for the image. These become input for parameters a , b , and c of the triangular membership function. The value returned by TFM ranges between 0 and 1, and clipping is done accordingly. Those intensity values that exceed the calculated clipping limit are redistributed as in CLAHE, thus resulting in a smoothed histogram. A triangular fuzzy number computed by the membership function is denoted by $TM = (a, b, c)$. The mathematical formulation of TFM is given by

$$\mu_1(Pr_\beta) = \begin{cases} 0 & Pr_\beta < a \\ \frac{Pr_\beta - a}{b - a} & a \leq Pr_\beta \leq b \\ \frac{c - Pr_\beta}{c - b} & b \leq Pr_\beta \leq c \\ 0 & Pr_\beta > c \end{cases} \tag{4}$$

Where the parameters $\{a, b, c\}$ (with $a < b < c$) determine $\mu_1(Pr_\beta)$ coordinates of the three corners of the underlying TFM. Here $\mu_1(Pr_\beta)$ denotes the image dependant clipping parameter. The point b , with a membership value of 1, is the mean value, and a and c are the left-hand spread and right-hand spread of Pr_β [33].

2.3. Different Applied Median Filter (DAMF)

Different Applied Median Filter (DAMF) in denoising process using grayscale images and get average values [27] with details step on below:

Step 1: Let $A := [a_{ij}]_{m \times n}$ be an image matrix (im) such that a_{ij} is an unsigned integer number, and $0 \leq a_{ij} \leq 255$. The a_{ij} is called a noisy entry of A if $a_{ij} = 0$ or $a_{ij} = 255$ otherwise a_{ij} is called a regular entry of A .

Step 2: Let A be an im . Then A is called a noise image matrix (nim) if for some i and j , a_{ij} is a noisy entry A .

Step 3: Let A be nim . Then the matrix $B := [b_{ij}]_{m \times n}$ is called the binary matrix of A where

$$B_{ij} = \begin{cases} 0, & a_{ij} \text{ is a noisy entry of } A \\ 1, & \text{Otherwise} \end{cases} \tag{5}$$

Step 4: Let $A := [a_{ij}]_{m \times n}$ and $t \in \{1, 2, \dots, \min\{m, n\}\}$. Then the matrix $P_A^t := [P_{rs}]_{(m+2t) \times (n+2t)}$ is called the t -symmetric pad matrix of A and is denoted as [27]

$$\begin{bmatrix} a_{tt} & \dots & a_{t1} & a_{t1} & a_{t2} & \dots & a_{tn} & a_{tn} & \dots & a_{t(n-t+1)} \\ \vdots & \ddots & \vdots & \vdots & \vdots & \ddots & \vdots & \vdots & \dots & \vdots \\ a_{1t} & \dots & a_{11} & a_{11} & a_{12} & \dots & a_{1n} & a_{1n} & \dots & a_{1(n-1+1)} \\ a_{1t} & \dots & a_{11} & a_{11} & a_{12} & \dots & a_{1n} & a_{1n} & \dots & a_{1(n-1+1)} \\ a_{2t} & \dots & a_{21} & a_{21} & a_{22} & \dots & a_{2n} & a_{2n} & \dots & a_{2(n-1+1)} \\ a_{3t} & \dots & a_{31} & a_{31} & a_{32} & \dots & a_{3n} & a_{3n} & \dots & a_{3(n-1+1)} \\ \vdots & \ddots & \vdots & \vdots & \vdots & \ddots & \vdots & \vdots & \dots & \vdots \\ a_{mt} & \dots & a_{m1} & a_{m1} & a_{m2} & \dots & a_{mn} & a_{mn} & \dots & a_{m(n-1+1)} \\ a_{mt} & \dots & a_{m1} & a_{m1} & a_{m2} & \dots & a_{mn} & a_{mn} & \dots & a_{m(n-1+1)} \\ \vdots & \ddots & \vdots & \vdots & \vdots & \ddots & \vdots & \vdots & \dots & \vdots \\ \vdots & \ddots & \vdots & \vdots & \vdots & \ddots & \vdots & \vdots & \dots & \vdots \\ a_{(m-t+1)t} & \dots & a_{(m-t+1)1} & a_{(m-t+1)1} & a_{(m-t+1)2} & \dots & a_{(m-t+1)n} & a_{(m-t+1)n} & \dots & a_{(m-t+1)(n-t)} \end{bmatrix} \tag{6}$$

Step 5: Let $A := [a_{ij}]_{m \times n}$, P_A^t be t -symmetric pad matrix of A and $k \in \{1, 2, \dots, t\}$. Then the matrix, denoted by A_{ij}^k , is called the k -approximate matrix of a_{ij} in P_A^t

$$\begin{bmatrix} P_{(i+t-k)(j+t-k)} & \cdots & P_{(i+t-k)(j+t+k)} \\ \vdots & P_{(i+t)(j+t)} & \vdots \\ P_{(i+t-k)(j+t-k)} & \cdots & P_{(i+t-k)(j+t+k)} \end{bmatrix}_{(2k+1) \times (2k+1)} \quad (7)$$

Step 6: Let A_{ij}^k be a k -approximate matrix. Then the matrix $H_{ij}^k = [h_{1u}]_{1 \times (2k+1)^2}$ consisting of all entries of A_{ij}^k and non-decreasing is called row matrix or entry matrix (*em*) of A_{ij}^k

Step 7: Let A_{ij}^k be a k -approximate matrix. Then the matrix $R_{ij}^k = [r_{1v}]$ consisting of all regular entries of A_{ij}^k and non-decreasing is called regular row matrix or regular entry (*rem*) of A_{ij}^k

Step 8: Let $R_{ij}^k = [r_{1v}]_{1 \times w}$ be the rem of A_{ij}^k the value

$$mR_{ij}^k := \left\{ \begin{array}{l} r_1(\frac{w+1}{2}), \quad \frac{w+1}{2} \in Z \\ \frac{1}{2}(r_{\frac{1}{2}w} + r_{1(\frac{w+2}{2})}), \quad \frac{w}{2} \in Z \end{array} \right\} \quad (8)$$

It is called media of R_{ij}^k

Step 9: A matrix with all its entries being zero is called a zero or null matrix and is denoted

2.4. Adaptive Fuzzy Contrast Enhancement with Details Preserving (AFCEDP)

The proposed AFCEDP algorithm comprises 4 stages as

1. Determination of the membership function
2. Computation of the degree of membership
3. Defining three plateau functions and computation of the clipping limit, and;
4. Clipping and equalization of the histogram

2.4.1. Determination of the membership function

The proposed AFCEDP technique defines a trapezoidal-shaped membership function at threshold values of 85 and 170. The membership functions for low-, middle- and high-level images, respectively, are shown as

$$\mu_{low}(k) = \begin{cases} 0, & \text{for } k > 95 \\ \frac{95-k}{20}, & \text{for } 75 \leq k \leq 95 \\ 1, & \text{for } k < 75 \end{cases}$$

$$\mu_{low}(k) = \begin{cases} 0, & \text{for } (k < 75) \cup (k > 180) \\ \frac{k-75}{20}, & \text{for } 75 \leq k \leq 95 \\ 1, & \text{for } 95 \leq k \leq 160 \\ \frac{180-k}{20}, & \text{for } 160 \leq k \leq 180 \end{cases} \quad (9)$$

$$\mu_{low}(k) = \begin{cases} 0, & \text{for } k < 160 \\ \frac{k-160}{20}, & \text{for } 160 \leq k \leq 180 \\ 1, & \text{for } k > 180 \end{cases}$$

where k is the intensity of the pixels in the image.

2.4.2. Computation of the Degree of Membership

In order to obtain the reference intensity for the trapezoidal membership function, the degree of belonging of an image to the three categories using partition is computed. The three categories, low-, middle- and high-level images, previously implemented in the conventional ACEDP, are used as reference. The image's reference intensity, λ , can be computed using Eq. (10).

$$\lambda = (low_part \times 43) + (mid_part \times 128) + (high_part \times 213) \quad (10)$$

2.4.3. Defining Three Plateau Functions and Computation of the Clipping Limit

The AFCEDP technique employs the same clipping functions as the conventional ACEDP technique. As described in the conventional ACEDP, the acceptable range for the slopes $c1$ and $c2$ is $[-0.015, -0.005]$

and [0.005, 0.007], respectively. In the proposed AFCEDP technique, the same values for c_1 and c_2 as employed in the conventional ACEDP technique are used for a fair comparison of the final results. The values for c_1 and c_2 are -0.01 and 0.007, respectively. Based on the reference intensity, λ , and the plateau functions, the AFCEDP technique implements the final clipping function, $(\sigma)k$, using Eq. (11)

$$\sigma(k) = [\mu_{low}(\lambda) \times level_{low}(k)] + [\mu_{mid}(\lambda) \times level_{mid}(k)] + [\mu_{high}(\lambda) \times level_{high}(k)] \quad (11)$$

2.4.4. Clipping and Equalization of the Histogram

The clipping function $\sigma(k)$ provides the clipping limit at each gray level. Consider an input grayscale image. The histogram of the image, $H(k)$, is defined as:

$$H(k) = n_k, \text{ for } k = 0, 1, \dots, L - 1 \quad (12)$$

Where n_k is the occurrence of intensity k in the image, and L is the total number of gray levels in the image. The probability density function (PDF) of the image $p(k)$ is defined as:

$$p(k) = \frac{H(k)}{N}, \text{ for } k = 0, 1, \dots, L - 1 \quad (13)$$

Where N is the total number of pixels in the image, the cumulative density function (CDF), $c(k)$ is defined as:

$$c(k) = \sum_{i=0}^k p(i), \text{ for } k = 0, 1, \dots, L - 1 \quad (14)$$

HE involves mapping input gray levels k into output gray level $f(k)$, where the transformation function $f(k)$ is defined as:

$$f(k) = X_0 + (X_{L-1} - X_0) \cdot c(k) \quad (15)$$

Where X_0 and X_{L-1} represent the lowest and highest gray levels, respectively. HE remaps the input image into the entire dynamic range $[X_0, X_{L-1}]$. In the proposed AFCEDP technique, the PDF of the input image is limited to the clipping function, as shown in Eq. (12)

$$new_p(k) = \min(p(k), \sigma(k)), \text{ for } k = 0, L - 1 \quad (16)$$

The CDF of the enhanced image can be computed using Eq. (13),

$$c(k) = \sum_{i=0}^k new_p(i), \text{ for } k = 0, 1, \dots, L - 1 \quad (17)$$

Finally, the transformation function of the AFCEDP technique can be represented in Eq. (15) and Eq. (17)

2.5. Measurement method

2.5.1. PSNR

The metric adopted to measure the signal-to-noise ratio of an image is the PSNR. Given the original infrared image I and the infrared image with enhancement I_{EN} where the size of the images is $M \times N$, the PSNR between I and I_{EN} is given by [37]

$$PSNR(I, I_E) = 10 * \log_{10} \left(\frac{L - 1^2}{MSE(I, I_E)} \right) \quad (18)$$

2.5.2. Mean Squared Error (MSE)

MSE is the most common estimator of image quality measurement metrics. It is a full reference metric, and the values closer to zero are better. It is the second moment of the error. The variance of the estimator and its bias are both incorporated with the mean squared error. The MSE is the variance of the estimator in the case of the unbiased estimator. It has the same units of measurement as the square of the quantity being calculated, like variance. The error is the difference between the estimator and the estimated outcome. It is a function of risk, considering the expected value of the squared error loss or quadratic loss. Mean Squared Error (MSE) between two images such as $I(u, v)$ and $I_{EN}(u, v)$ is defined as [37]:

$$MSE(I, I_E) = \frac{1}{M \times N} \sum_{u=0}^{M-1} \sum_{v=0}^{N-1} (I(u, v) - I_{EN}(u, v))^2 \quad (19)$$

2.5.3. Shannon Entropy (SE)

In the field of information theory, entropy, also called the entropy of information and Shannon's entropy, measures the uncertainty of a source of information [38]. The Shannon entropy can measure the uncertainty of a random process. Rolling element machinery without failure tends to generate a more random signal, and the machine with failure usually tends to have a more deterministic signal; i.e., the Shannon entropy will be different [39]. Shannon's entropy is defined as:


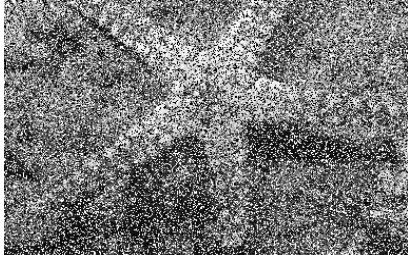



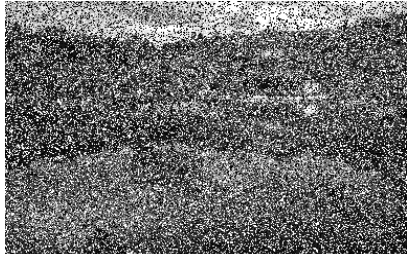

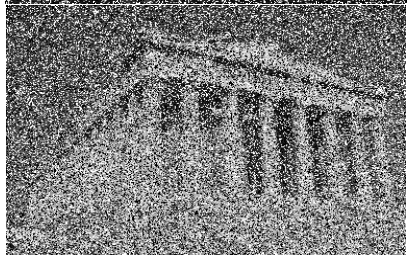
$$E = - \sum_{i=0}^N p_i \text{Log } p_i \quad (20)$$


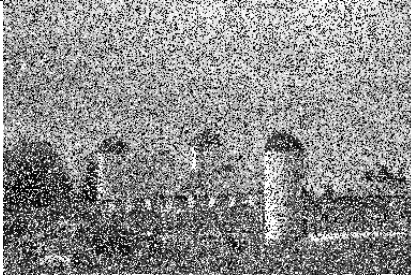



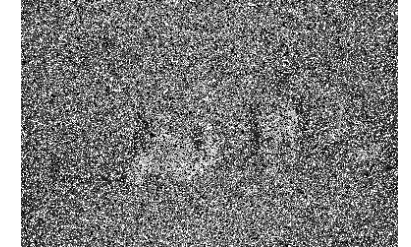



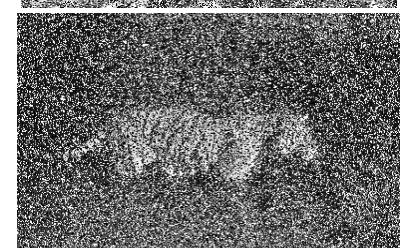


Where N is the total number of observed events, and p_i is the probability of the i event.

2.6. Dataset

According to many objects in all datasets, then choose to use 10 images that represent distribution objects in images. The dataset used in this study is taken from the Brno University of Technology website [40] with as many as 10 images in grayscale. Table 1 presents a brief description of the dataset used in this study. All of the datasets in Table 1 are images of PNG extension with the percentage of salt and pepper noise in the amount of 45%.

Table 1. Dataset

No.	Name	Original Images	Images with 45% Noise
1.	Image-1.png		
2.	Image-2.png		
3.	Image-3.png		
4.	Image-4.png		

No.	Name	Original Images	Images with 45% Noise
5.	Image-5.png		
6.	Image-6.png		
7.	Image-7.png		
8.	Image-8.png		
9.	Image-9.png		
10.	Image-10.png		

2.7. Research method

This research is experimental research to find out the best combination of some algorithms for denoising and contrast enhancement using measurement of this combination with PSNR and Shannon Entropy values. The research steps are presented in [Fig. 1](#).

3. RESULTS AND DISCUSSION

The main process of this research using the combinations of methods is to reduce noise and increase the contrast of images of the dataset. The dataset in [Table 1](#) is denoising and contrast enhancement using IDBP-CNN and DAMF algorithms. After that, improve contrast enhancement using TFM-Clahe and AFCEDP algorithm. The results of the reduction and contrast enhancement will be compared to the original image, which improves contrast enhancement too, just to make a fair result that is shown in [Fig. 1](#).

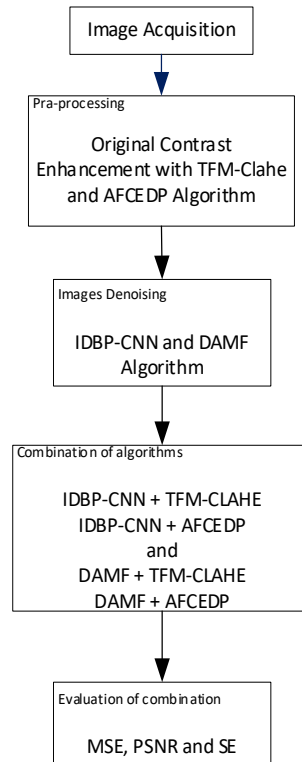


Fig. 1. Research flowchart

Explanation of flowchart in [Fig. 1](#), showed process start with Image Acquisition of grayscale images 45% noise, and in pra-processing to purpose to get fairness of measurement PSNR comparing original image and result in images, need to enhanced contrast with TFM-Clahe and AFCEDP algorithm, next step is denoising images with IDBP-CNN and DAMF algorithm, and continue solving low contrast with combine TFM-Clahe and AFCEDP algorithm, at the end of step get measurement quality of images to result with PSNR and SE.

The main objective of this research is to find out the best combination of denoising and contrast enhancement algorithm based on PSNR and SE values with a combination of:

- a) IDBP-CNN algorithm + TFM-Clahe algorithm
- b) IDBP-CNN algorithm + AFCEDP algorithm
- c) DAMF algorithm + TFM-Clahe algorithm
- d) DAMF algorithm + AFCEDP algorithm

[Fig. 1](#) is shown the original images, which are low-contrast images that need to get pre-processing to implement contrast enhancement with TFM-Clahe and AFCEDP to get a fair result image before getting measurement using PSNR and Shannon entropy according to the deviation of original and result image. [Table 2](#) and [Table 3](#) show the result of implementing the algorithm combination according to the testing scenario to denoising 45% noise salt and contrast enhancement as shown in the table.

3.1. Combination of IDBP-CNN algorithm and TFM-Clahe algorithm (IDBP-CNN + TFM-Clahe)

The first combination of experimental to solve problem noise with 45% and low contrast of images using IDBP-CNN + TFM-Clahe get the result shown in [Fig. 2](#) with the quality of Images according to PSNR is above 32.60 dB. The best quality of images in Image 5 by PSNR value 34.60 dB and average deviation of information image using Shannon entropy are 0.061.

Table 2. Result of implementation of combining algorithm-1

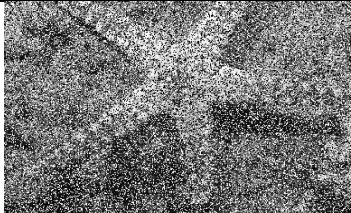

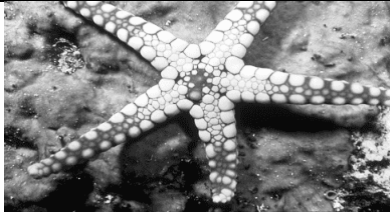
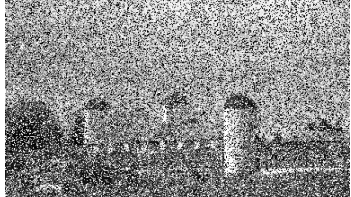


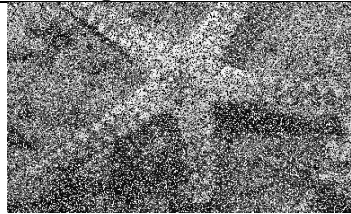
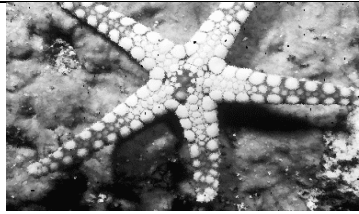
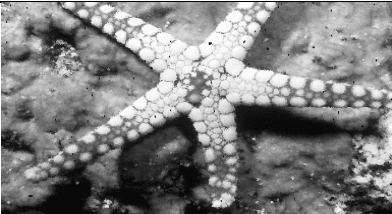
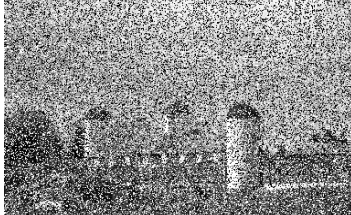


Images with 45% Noise	IDBP-CNN+TFM Clahe	IDBP-CNN+AFCEDP
		
		

Table 3. Result of implementation of combining algorithm-2

Images with 45% Noise	DAMF+TFM CLAhe	DAMF + AFCEDP
		
		

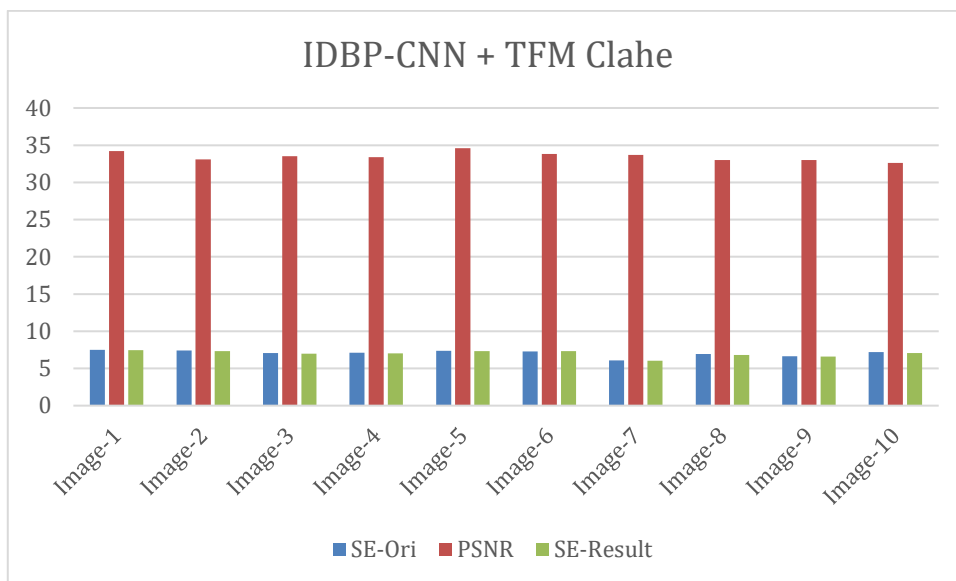


Fig. 2. Result of combination IDBP-CNN + TFM Clahe algorithm

3.2. Combination of DAMF algorithm and TFM-Clahe algorithm (DAMF + TFM-Clahe)

The second combination experimental was tested to solve noise with 45% and low contrast of images using DAMF + TFM Clahe. The result shown in Fig. 3 with quality of Images according to PSNR is above 34.00 dB, and the best quality of images in Image 5 by PSNR value 35.90 dB and average deviation of information image are 0.014.

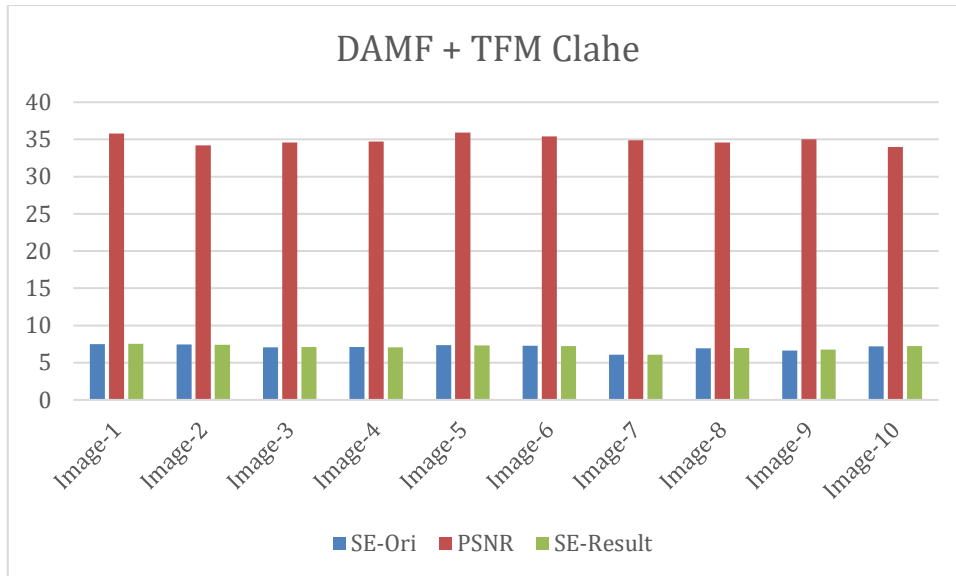


Fig. 3. Result of combination DAMF + TFM Clahe algorithm

3.3. Combination of DAMF algorithm and AFCDEP algorithm (DAMF + AFCDEP)

Third combination, experimental was tested to solve noise with 45% and low contrast of images using DAMF + AFCDEP. The result shown in Fig. 4 with the quality of Images according to PSNR is above 33.90 dB, and the best quality of images in Image 5 by PSNR value 35.90 dB and average deviation of information image are 0.014.

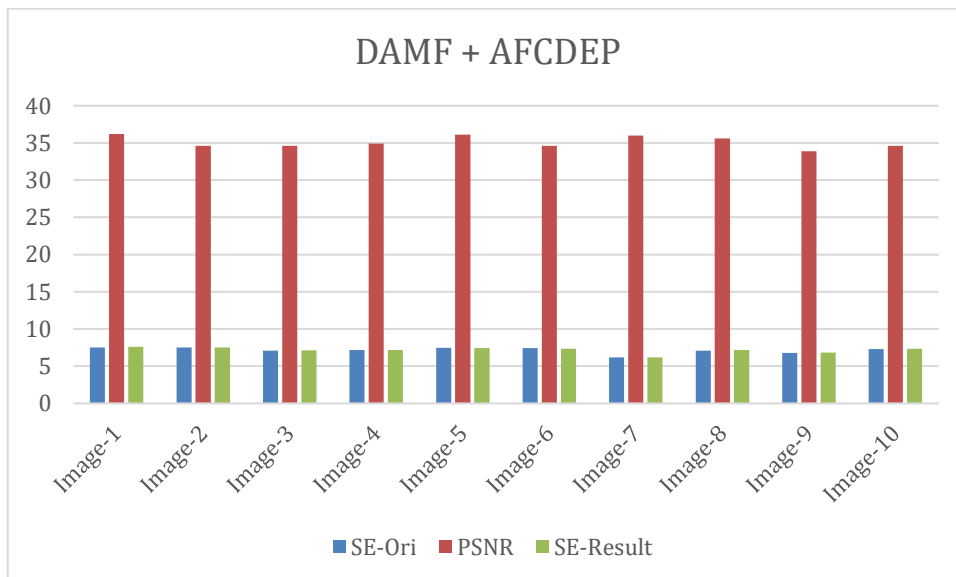


Fig. 4. Result of combination DAMF + AFCDEP algorithm

3.4. Combination of IDBP-CNN algorithm and AFCDEP algorithm (IDBP-CNN + AFCDEP-Clahe)

The last combination experimental was tested to solve noise with 45% and low contrast of images using DAMF + AFCDEP. The result shown in Fig. 5 with quality of Images according to PSNR is above 33.10 dB, and the best quality of images in Image 1 by PSNR value 42.20 dB and average deviation of information image is 0.088.

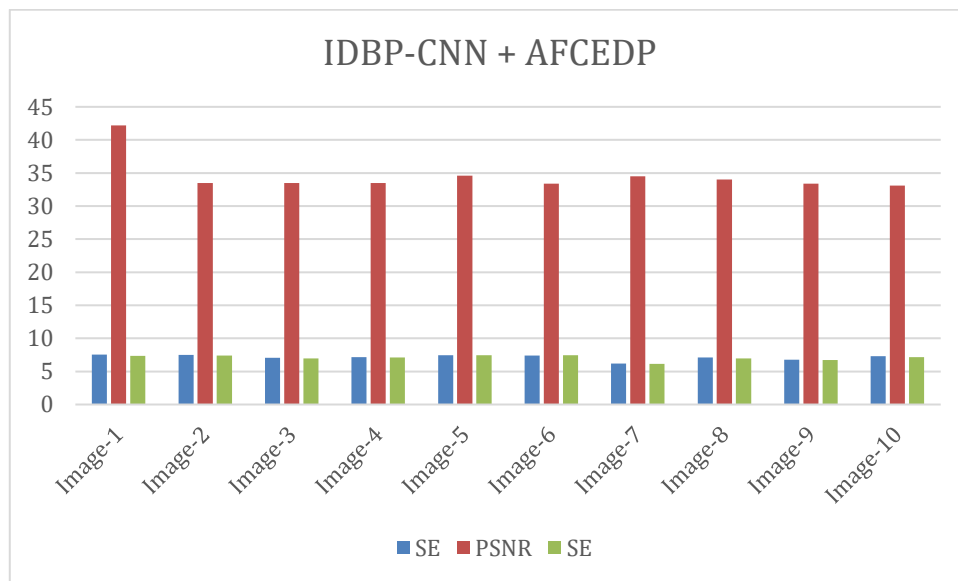


Fig. 5. Result of IDBP-CNN + AFCEDP algorithm

The result of the PSNR value of each image is not convergent at all. There are some different results for each image to every combination, so to get the best conclusion is to get the average of the all-image result, and comparing to one-by-one combination, and get the value of the detail shown in Table 4.

Table 4 is shown a combination of the DAMF algorithm and AFCEDP algorithm to get the best result image with an average of PSNR 35.11 dB, and the average difference information of the original image with the resulting image is 0.013 is the lowest rather than the other combination. Then following, combined with the best result, the DAMF algorithm continues TFM Clahe get PSNR 34.91 dB, and combination IDBP-CNN algorithm with AFCEDP get PSNR is 34.57 dB, and IDBP-CNN algorithm continues TFM Clahe algorithm get PSNR 33.49 dB. Quality of image based on Shannon entropy value is best in DAMF algorithm to continue AFCEDP combination with differential 0.013, following the combination of the other DAMF algorithm continue TFM Clahe algorithm is 0.014, IDBP-CNN algorithm continue TFM Clahe algorithm is 0.061, and the last combination IDBP-CNN algorithm continue AFCEDP algorithm is 0.088. In Table 4, the combination of IDBP-CNN continues AFCEDP algorithm get the best result image quality with PSNR 42.20 dB.

Table 4. Result of combination algorithm

Name	Ori + TFM		IDBP-CNN + TFM Clahe		DAMF + TFM Clahe		Ori + AFCEDP		DAMF + AFCEDP		IDBP-CNN + AFCEDP	
	SE	PSNR	SE	PSNR	SE	PSNR	SE	PSNR	SE	PSNR	SE	
Image-1	7.48	34.20	7.45	35.80	7.51	7.53	36.20	7.58	42.20	7.37		
Image-2	7.43	33.10	7.34	34.20	7.42	7.51	34.60	7.51	33.50	7.42		
Image-3	7.06	33.50	6.97	34.60	7.10	7.07	34.60	7.12	33.50	6.99		
Image-4	7.11	33.40	7.01	34.70	7.06	7.18	34.90	7.16	33.50	7.10		
Image-5	7.35	34.60	7.32	35.90	7.32	7.46	36.10	7.45	34.60	7.44		
Image-6	7.29	33.80	7.33	35.40	7.24	7.42	34.60	7.35	33.40	7.45		
Image-7	6.06	33.70	6.03	34.90	6.06	6.19	36.00	6.18	34.50	6.14		
Image-8	6.93	33.00	6.82	34.60	6.99	7.10	35.60	7.16	34.00	6.98		
Image-9	6.65	33.00	6.59	35.00	6.75	6.79	33.90	6.81	33.40	6.71		
Image-10	7.19	32.60	7.07	34.00	7.23	7.29	34.60	7.33	33.10	7.18		
Average	7.05	33.49	6.99	34.91	7.07	7.15	35.11	7.17	34.57	7.08		
Deviation			0.061		0.014			0.013		0.088		

4. CONCLUSION

Based according of all tests, the best combination algorithm for denoising and contrast enhancement is the DAMF algorithm, which continues with the AFCEDP algorithm, which an average of PSNR is 35.11dB. The difference between the Shannon entropy original image and result image is 0.013, and the opposite, the worst combination is the IDBP-CNN algorithm and continues with the TFM Clahe algorithm, which an average of PSNR 33.49. The worst difference in information image using Shannon entropy is the

combination IDBP-CNN algorithm with the AFCEDP algorithm with a value of 0.088. In the future, research needs further on the development of processes to identify the object with implementation method to low contrast and noise of medical images.

Acknowledgments

The author would like to thank the Ministry of Research and Technology for the assistance provided funding to complete this paper through the 2020 Grants and Mikroskil University for supporting as long progressing this paper until to publish.

REFERENCES

- [1] J. R. Tang and N. A. M. Isa, "An Adaptive Fuzzy Contrast Enhancement Algorithm with Details Preserving," *J. ICT Res. Appl.*, vol. 8, no. 2, pp. 126–140, Dec. 2014, <https://doi.org/10.5614/itbj.ict.res.appl.2014.8.2.4>.
- [2] Y. Zhou, C. Shi, B. Lai, and G. Jimenez, "Contrast enhancement of medical images using a new version of the World Cup Optimization algorithm," *Quant. Imaging Med. Surg.*, vol. 9, no. 9, pp. 1528–1547, Sep. 2019, <https://doi.org/10.21037/qims.2019.08.19>.
- [3] B. Subramani and M. Veluchamy, "Fuzzy contextual inference system for medical image enhancement," *Measurement*, vol. 148, p. 106967, Dec. 2019, <https://doi.org/10.1016/j.measurement.2019.106967>.
- [4] M. Pitchammal, S. S. Nisha, and M. M. Sathik, "Noise Reduction in MRI Neck Image Using Adaptive Fuzzy Filter in Contourlet Transform," *Int. J. Eng. Sci. Comput.*, vol. 6, no. 3, pp. 2478–2484, 2016.
- [5] K. Mayathevar, M. Veluchamy, and B. Subramani, "Fuzzy color histogram equalization with weighted distribution for image enhancement," *Optik (Stuttg.)*, vol. 216, no. May, p. 164927, Aug. 2020, <https://doi.org/10.1016/j.ijleo.2020.164927>.
- [6] Z. Zhao and X. Gao, "Image Contrast Enhancement Method Based on Nonlinear Space and Space Constraints," *Wirel. Commun. Mob. Comput.*, vol. 2022, pp. 1–9, Feb. 2022, <https://doi.org/10.1155/2022/2572523>.
- [7] S. Gupta and R. K. Sunkaria, "Real-time salt and pepper noise removal from medical images using a modified weighted average filtering," in *2017 Fourth International Conference on Image Information Processing (ICIIP)*, Dec. 2017, vol. 2018-Maret, pp. 1–6, <https://doi.org/10.1109/ICIIP.2017.8313718>.
- [8] S. Asnani, M. G. Canu, L. Farinetti, and B. Montrucchio, "On producing energy-efficient and contrast-enhanced images for OLED-based mobile devices," *Pervasive Mob. Comput.*, vol. 75, p. 101384, Aug. 2021, <https://doi.org/10.1016/j.pmcj.2021.101384>.
- [9] T. Gebreyohannes, "Adaptive Noise Reduction Scheme for Salt and Pepper," *Signal Image Process. An Int. J.*, vol. 2, no. 4, pp. 47–55, Dec. 2011, <https://doi.org/10.5121/sipij.2011.2405>.
- [10] E. J. Leavline and D. A. A. G. Singh, "Salt and Pepper Noise Detection and Removal in Gray Scale Images: An Experimental Analysis," *Int. J. Signal Process. Image Process. Pattern Recognit.*, vol. 6, no. 5, pp. 343–352, Oct. 2013, <https://doi.org/10.14257/ijsp.2013.6.5.30>.
- [11] C. Tian, Y. Xu, W. Zuo, B. Du, C.-W. Lin, and D. Zhang, "Designing and training of a dual CNN for image denoising," *Knowledge-Based Syst.*, vol. 226, p. 106949, Aug. 2021, <https://doi.org/10.1016/j.knsys.2021.106949>.
- [12] I. A. Pardosi and H. Gohzali, "Peningkatan Kualitas Citra Reduksi Noise Menggunakan Iterative Denoising and Backward Projection-CNN dan TFM-CLAHE Pada Citra 24 Bit," *Techno.Com*, vol. 20, no. 4, pp. 566–578, Nov. 2021, <https://doi.org/10.33633/tc.v20i4.5243>.
- [13] I. A. Pardosi and A. A. Lubis, "Analisis Kualitas Citra Hasil Reduksi Noise Menggunakan Spatial Median Filter dan Adaptive Fuzzy Filter Terhadap Variasi Kedalaman Citra," *Indones. J. Inf. Syst.*, vol. 1, no. 2, p. 78, Feb. 2019, <https://doi.org/10.24002/ijis.v1i2.1939>.
- [14] L. Liang, S. Deng, L. Gueguen, M. Wei, X. Wu, and J. Qin, "Convolutional neural network with median layers for denoising salt-and-pepper contaminations," *Neurocomputing*, vol. 442, pp. 26–35, Jun. 2021, <https://doi.org/10.1016/j.neucom.2021.02.010>.
- [15] S. Malik and R. Soundararajan, "A low light natural image statistical model for joint contrast enhancement and denoising," *Signal Process. Image Commun.*, vol. 99, no. February 2020, p. 116433, Nov. 2021, <https://doi.org/10.1016/j.image.2021.116433>.
- [16] A. Saleh Ahmed, W. H. El-Behaidy, and A. A. A. Youssif, "Medical image denoising system based on stacked convolutional autoencoder for enhancing 2-dimensional gel electrophoresis noise reduction," *Biomed. Signal Process. Control*, vol. 69, no. January, p. 102842, Aug. 2021, <https://doi.org/10.1016/j.bspc.2021.102842>.
- [17] K. Srinivas, A. K. Bhandari, and A. Singh, "Low-contrast image enhancement using spatial contextual similarity histogram computation and color reconstruction," *J. Franklin Inst.*, vol. 357, no. 18, pp. 13941–13963, Dec. 2020, <https://doi.org/10.1016/j.jfranklin.2020.10.013>.
- [18] H. Singh, S. V. R. Kommuri, A. Kumar, and V. Bajaj, "A new technique for guided filter based image denoising using modified cuckoo search optimization," *Expert Syst. Appl.*, vol. 176, no. November 2019, p. 114884, Aug. 2021, <https://doi.org/10.1016/j.eswa.2021.114884>.
- [19] M. Sindhana Devi and M. Soranamageswari, "Efficient impulse noise removal using hybrid neuro-fuzzy filter with optimized intelligent water drop technique," *Int. J. Imaging Syst. Technol.*, vol. 29, no. 4, pp. 465–475, 2019, <https://doi.org/10.1002/ima.22324>.
- [20] M. Nadeem, A. Hussain, A. Munir, M. Habib, and M. T. Naseem, "Removal of random valued impulse noise from grayscale images using quadrant based spatially adaptive fuzzy filter," *Signal Processing*, vol. 169, p. 107403, Apr.

- 2020, <https://doi.org/10.1016/j.sigpro.2019.107403>.
- [21] R. C. Gonzalez, R. E. Woods, and B. R. Masters, "Digital Image Processing, Third Edition," *J. Biomed. Opt.*, vol. 14, no. 2, p. 029901, 2009, <https://doi.org/10.1117/1.3115362>.
- [22] I. A. Pardosi *et al.*, "Restorasi Citra Digital Menggunakan Iterative Denoising dan Backward Projections with CNN," *SIFO Mikroskil*, vol. 21, no. 1, pp. 37–50, 2020, <https://www.mikroskil.ac.id/ejurnal/index.php/jsm/article/view/721>.
- [23] R. Hou and F. Li, "IDPCNN: Iterative denoising and projecting CNN for MRI reconstruction," *J. Comput. Appl. Math.*, vol. 406, p. 113973, May 2022, <https://doi.org/10.1016/J.CAM.2021.113973>.
- [24] G. M. Daiyan and M. A. Mottalib, "Removal of high density salt & pepper noise through a modified decision based median filter," in *2012 International Conference on Informatics, Electronics & Vision (ICIEV)*, May 2012, vol. 18, no. 5, pp. 565–570, <https://doi.org/10.1109/ICIEV.2012.6317448>.
- [25] C. J. J. Sheela and G. Suganthi, "An efficient denoising of impulse noise from MRI using adaptive switching modified decision based unsymmetric trimmed median filter," *Biomed. Signal Process. Control*, vol. 55, 2020, <https://doi.org/10.1016/j.bspc.2019.101657>.
- [26] B. R. Jana, H. Thotakura, A. Baliyan, M. Sankararao, R. G. Deshmukh, and S. R. Karanam, "Pixel density based trimmed median filter for removal of noise from surface image," *Appl. Nanosci.*, 2021, <https://doi.org/10.1007/s13204-021-01950-0>.
- [27] U. Erkan, L. Gökrem, and S. Enginoğlu, "Different applied median filter in salt and pepper noise," *Comput. Electr. Eng.*, vol. 70, pp. 789–798, Aug. 2018, <https://doi.org/10.1016/j.compeleceng.2018.01.019>.
- [28] Q. Wang and S. Bi, "Prediction of the PSNR Quality of Decoded Images in Fractal Image Coding," *Math. Probl. Eng.*, vol. 2016, pp. 1–13, 2016, <https://doi.org/10.1155/2016/2159703>.
- [29] H. Sajati, "Analisis Kualitas Perbaikan Citra Menggunakan Metode Median Filter Dengan Penyeleksian Nilai Pixel," *Angkasa J. Ilm. Bid. Teknol.*, vol. 10, no. 1, p. 41, May 2018, <https://doi.org/10.28989/angkasa.v10i1.223>.
- [30] S. Anwar and G. Rajamohan, "Improved Image Enhancement Algorithms based on the Switching Median Filtering Technique," *Arab. J. Sci. Eng.*, vol. 45, no. 12, pp. 11103–11114, Dec. 2020, <https://doi.org/10.1007/s13369-020-04983-9>.
- [31] I. A. Pardosi, P. Sirait, S. Goh, and R. Chandra, "Perbaikan Citra Gelap dan Pembesaran Objek Citra Menggunakan Gradient Based Low-Light Image Enhancement dan Rational Ball Cubic B-Spline With Genetic Algorithm," *J. SIFO Mikroskil*, vol. 20, no. 2, pp. 105–115, 2019, <https://www.mikroskil.ac.id/ejurnal/index.php/jsm/article/view/674>.
- [32] M. Tanaka, T. Shibata, and M. Okutomi, "Gradient-Based Low-Light Image Enhancement," in *2019 IEEE International Conference on Consumer Electronics (ICCE)*, Jan. 2019, pp. 1–2, <https://doi.org/10.1109/ICCE.2019.8662059>.
- [33] B. Sree Vidya and E. Chandra, "Triangular Fuzzy Membership-Contrast Limited Adaptive Histogram Equalization (TFM-CLAHE) for Enhancement of Multimodal Biometric Images," *Wirel. Pers. Commun.*, vol. 106, no. 2, pp. 651–680, May 2019, <https://doi.org/10.1007/s11277-019-06184-6>.
- [34] J. Joseph, J. Sivaraman, R. Periyasamy, and V. R. Simi, "An objective method to identify optimum clip-limit and histogram specification of contrast limited adaptive histogram equalization for MR images," *Biocybern. Biomed. Eng.*, vol. 37, no. 3, pp. 489–497, 2017, <https://doi.org/10.1016/j.bbe.2016.11.006>.
- [35] W. Zhang, X. Pan, X. Xie, L. Li, Z. Wang, and C. Han, "Color correction and adaptive contrast enhancement for underwater image enhancement," *Comput. Electr. Eng.*, vol. 91, no. December 2020, p. 106981, May 2021, <https://doi.org/10.1016/j.compeleceng.2021.106981>.
- [36] T. Tirer and R. Giryes, "Image Restoration by Iterative Denoising and Backward Projections," *IEEE Trans. Image Process.*, vol. 28, no. 3, pp. 1220–1234, Mar. 2019, <https://doi.org/10.1109/TIP.2018.2875569>.
- [37] U. Sara, M. Akter, and M. S. Uddin, "Image Quality Assessment through FSIM, SSIM, MSE and PSNR—A Comparative Study," *J. Comput. Commun.*, vol. 7, no. 3, pp. 8–18, 2019, <https://doi.org/10.4236/jcc.2019.73002>.
- [38] J. Mello Román, J. Vázquez Noguera, H. Legal-Ayala, D. Pinto-Roa, S. Gomez-Guerrero, and M. García Torres, "Entropy and Contrast Enhancement of Infrared Thermal Images Using the Multiscale Top-Hat Transform," *Entropy*, vol. 21, no. 3, p. 244, Mar. 2019, <https://doi.org/10.3390/e21030244>.
- [39] D. Galar and U. Kumar, "Preprocessing and Features," in *eMaintenance*, 2017, pp. 129–177, <https://doi.org/10.1016/B978-0-12-811153-6.00003-8>.
- [40] Z. Vašiček, "45% salt-and-pepper noise," *Brno University of Technology*, <http://www.fit.vutbr.cz/~vasicek/imagedb/?lev=45&knd=corrupted>.